The Food-Associated Ribotoxin Deoxynivalenol Modulates Inducible NO Synthase in Human Intestinal Cell Model

Fabien Graziani, Ange Pujol, Cendrine Nicoletti, Philippe Pinton, Loriane Armand, Eric Di Pasquale, Isabelle P. Oswald, Josette Perrier, Marc Maresca

The food-associated ribotoxin deoxynivalenol modulates inducible NO synthase in human intestinal cell model.

Running title: Deoxynivalenol induces iNOS degradation.

Fabien Graziani*,¶, Ange Pujol*,¶, Cendrine Nicoletti*, Philippe Pinton†, Loriane Armand*, Eric Di Pasquale‡, Isabelle P. Oswald†, Josette Perrier*, Marc Maresca*,#.

* Aix Marseille Université, Centrale Marseille, CNRS, iSm2 UMR 7313,13397, Marseille, France

† INRA, UMR1331, Toxalim, Research Centre in Food Toxicology, F-31027, Toulouse, France. Université de Toulouse, INP, UMR1331, Toxalim, F-31000, Toulouse, France

‡ Aix Marseille Université, CNRS, CRN2M UMR 7286, 13344, Marseille, France

¶ F.G and A.P contributed equally to this work

To whom correspondence should be addressed. Dr Marc Maresca. Aix Marseille Université, Centrale Marseille, CNRS, iSm2 UMR 7313,13397, Marseille, France. E-mail: m.maresca@univ-amu.fr. Phone: +33 4 91 28 82 54. Fax: +33 4 91 28 84 40.

Abstract

The intestinal epithelium possesses active immune functions including the production of proinflammatory cytokines and antimicrobial molecules such as nitric oxide (NO). As observed with immune cells, the production of NO by the intestinal epithelium is mainly due to the expression of the inducible NO synthase (iNOS or NOS2). Epithelial immune functions could be affected by many factors including pathogenic microorganisms and food-associated toxins (bacterial and fungal). Among the various mycotoxins, deoxynivalenol (DON) is known to alter the systemic and intestinal immunity. However, little is known about the effect of DON on the production of NO by the intestinal epithelium. We studied the impact of DON on the intestinal expression of iNOS using the Caco-2 cell model. In line with its proinflammatory activity, we observed that DON dose-dependently up-regulates the expression of iNOS mRNA. Surprisingly, DON failed to increase the expression of iNOS protein. When testing the effects of DON on cytokine-mediated induction of iNOS, we found that very low concentrations of DON (i.e. 1 µM) decrease the amount of iNOS protein but not of iNOS mRNA. We demonstrated that DON's effect on iNOS protein relies on its ability to activate signal pathways and to increase iNOS ubiquitinylation and degradation through the proteasome pathway. Taken together, our results demonstrate that although DON causes intestinal inflammation, it suppresses the ability of the gut epithelium to express iNOS and to produce NO, potentially explaining the increased susceptibility of animals to intestinal infection following exposure to low doses of DON.

Keywords: deoxynivalenol, iNOS, intestinal immunity, mycotoxin, nitric oxide, trichothecene.

Introduction

The intestinal epithelium is continuously exposed to noxious molecules and micro-organisms present in the food ingested daily. Both passive and active strategies have been developed to maintain the intestinal immunity (Kagnoff, 2014; Moens and Veldhoen, 2012; Santaolalla and Abreu, 2012). The intestinal epithelial cells (IEC) tightly linked together by tight junctions and covered by the mucus layer are responsible for the passive defense of the gut. In addition, the protection of the gut epithelium also relies on active mechanisms such as the secretion by the IEC of pro-inflammatory cytokines and of various anti-microbial molecules, including nitric oxide (Elliott and Wallace, 1998; Moens and Veldhoen, 2012). Nitric oxide (NO) is generated by nitric oxide synthase (NOS)-mediated conversion of L–arginine to L-citrulline . While several forms of NOS exist (constitutive, endothelial and inducible; cNOS, eNOS and iNOS respectively) only iNOS (or NOS2) plays an immune role related to its ability to produce large amounts of NO over long periods of time (Elliott and Wallace, 1998). Like immune cells, IEC are able to express iNOS following exposure to pro-inflammatory cytokines and / or to bacteria (Maresca et al., 2005; Salzman et al., 1998; Witthoft et al., 1998). Although long-term production of NO could be deleterious, intestinal iNOS activity is considered to be beneficial in relation to its antimicrobial activity (Elliott and Wallace, 1998). The importance of iNOS in gut immunity was illustrated by the finding that iNOS-deficient mice are more susceptible to intestinal infection (Alam *et al*., 2002; Elliott and Wallace, 1998) and by the fact that various pathogenic bacteria (including *Citrobacter rodentium* and enteropathogenic *E coli*) have developed strategies to inhibit iNOS induction (Maresca et al., 2005, Vallance et al., 2002).

In addition to pathogenic micro-organisms, the gut is daily exposed to harmful chemicals and molecules present in the food, such as pesticides, heavy metals or mycotoxins (Mattsson, 2007). Mycotoxins are structurally non-related secondary metabolites produced by various molds such as *Aspergillus, Penicillium* or *Fusarium* species (Wu et al., 2014a). Among the large number of existing mycotoxins, i.e. more than 350 (Mattsson, 2007), some have attracted special attention, such as deoxynivalenol (DON). DON belongs to a family of mycotoxins called trichothecenes. Trichothecenes are small sesquiterpenoid with an epoxide group at position 12-13 allowing their binding to ribosomes. This leads to the activation of various protein kinases, the modulation of gene expression, the inhibition of the synthesis of proteins and to general cell toxicity (Arunachalam and Doohan, 2013; Maresca, 2013; Pestka, 2010). In addition to cause anorectic and emetic effect (Wu et al., 2014b), exposure to DON has been associated to alterations of the intestinal, immune and brain cell functions (Awad et al., 2013; Maresca, 2013; Pestka, 2010; Pinton and Oswald, 2014; Razafimanjato et al., 2011). DON effects on immune cells are well documented, its ingestion being associated to alterations of the expression of proinflammatory cytokines and inflammation in different organs, including the liver (Gerez et al., 2014; Pestka, 2010; Wu et al., 2014c). The effects of DON on animal and human IEC functions are also well described. DON is known for example to alter the barrier function, to modify the intestinal immunity and the microbiota and to increase the susceptibility of animals to intestinal infection (Antonissen et al., 2014; Bouhet and Oswald, 2005; Cano et al., 2013; Ghareeb et al., 2014; Maresca, 2013; Pinton and Oswald, 2014; Saint-Cyr et al., 2013). Such observations lead us, since 2010, to make the hypothesis of a direct link between the oral exposure to mycotoxins and human inflammatory bowel diseases (IBD) such as Crohn's disease

(Maresca and Fantini, 2010). Although DON affects gut immunity, its effect on intestinal expression of iNOS has been poorly characterized. In a pioneer study, Gajęcki's group shown that DON modulates the intestinal expression of iNOS mRNA in pig (Gajęcka et al., 2013). Unfortunately, this study did not define if the observed modulation of iNOS mRNA was followed by an effect on iNOS protein expression and NO production, if this effect was direct or indirect (i.e. through the induction of intestinal inflammation for example) or if such effect could be observed in humans at low concentrations of DON susceptible to be present in food. In the present study, we studied if DON affects the expression of iNOS (mRNA, protein and NO production) by human IEC.

Materials and Methods

Cell culture.

Parental Caco-2 cells (from ATCC) were routinely grown in Dulbecco's modified essential medium (DMEM) supplemented with 10 % fetal calf serum (FCS), 1 % L-glutamine and 1% antibiotics (all from Invitrogen) and maintained in a 5 % CO2 incubator at 37 °C. For studying DON effects, Caco-2 cells were seeded at a density of 250,000 cells per cm^2 onto Greiner inserts (ThinCert™) (1 cm^2 or 4.5 cm^2 area, 3 µm pore size) and left to differentiate with medium changed every 2 days. After 10 to 14 days of differentiation, epithelial tightness and cellular differentiation were evaluated by measurement of the transepithelial electrical resistance (TER) using a voltohmmeter (Millipore). Only tight inserts with a TER superior or equal to 150 Ωcm^2 were used.

Mycotoxin treatment and cell viability measurement.

DON (from Romer Lab) stock solutions was prepared in anhydrous ethanol and stored at −20 °C. Serial dilutions of DON were prepared in anhydrous ethanol allowing the addition of similar volume of vehicle in all experiments. Caco-2 cells seeded onto inserts were treated with the indicated concentrations of DON or equivalent volume of ethanol (untreated cells) (1 % final, volume/volume). To mimic the physiological situation, DON was added apically in 0.5 ml of FCS and antibiotics-free DMEM, the basolateral compartment being filled with 1 ml of DMEM supplemented with 10 % FCS but no antibiotics. Viability of Caco-2 cells was evaluated by measuring the release of the cytosolic enzyme lactate dehydrogenase (LDH) using a home-made LDH assay (Razafimanjato et al., 2010, 2011). Briefly, 50 µl of culture supernatants were added to 250 µl of reaction buffer containing: Tris-HCl (86 mM; pH 9.3); KCl (172 mM); L-lactic acid (56 mM), and NAD (6.88 mM) in 96-wells microplates. OD at 340 nm was measured 30 s after culture supernatants were added to wells giving the initial measure. OD340 nm was then measured after 10 min of incubation at 37 °C, variation of OD being linear over this time period (data not shown). Percentage of released LDH was then calculated using culture supernatant of cells treated with Triton-X100 (1 % final concentration) corresponding to 100 % of release.

Induction of iNOS expression by pro-inflammatory cytokines.

Expression of iNOS was induced using a cocktail of pro-inflammatory cytokines as previously described (Maresca et al., 2005). Briefly, Caco-2 cells seeded onto inserts and treated or not with DON were incubated 24 h in the presence of a cocktail of human recombinant inflammatory cytokines (called cytomix) composed of IFN-γ (2000 $U.ml^{-1}$ final concentration), TNF-α (100 $ng.ml^{-1}$ final concentration) and IL-1β (5

ng.ml^{-1} final concentration) all purchased from Peprotech. To mimic the physiological situation, cytomix was added basolaterally to Caco-2 inserts. In some experiments, inhibitors were also added to investigate the role of proteasome and signal pathways in DON effect (all from Tocris, France).

Measurement of interleukin-8 secretion.

The secretion of IL-8 by Caco-2 cells exposed to DON and cytomix was measured as previously described (Maresca et al., 2008) using commercial ELISA kit (OptEIA human IL-8 from BD Biosciences, France).

Quantification of iNOS mRNA.

Caco-2 inserts (1 cm^2) were washed three times with sterile PBS and cells were lysed on ice using 500 µl of Tri reagent (Molecular Research Center). Thereafter total RNA was extracted using the RNeasy® miniKit (QIAGEN®) following the manufacturer's protocol. RNA concentrations were quantified at 260 nm using Nanodrop™ spectrophotometer and purity was assessed by the $A_{260}/A_{280\ nm}$ ratio. Reverse transcription was performed using SuperScript® VILO™ cDNA synthesis kit (Invitrogen™) according to the manufacturer's instructions and gene expression analysis was carried out using quantitative real-time PCR (qPCR) on a LightCycler® 480 instrument II (Roche applied science). 25 ng of total cDNA were incubated in the presence of LightCycler® 480 SYBR Green I Master (Roche applied science) and 0.5 µM of each primer. Primers used for iNOS and GAPDH mRNA quantification were selected using Universal ProbeLibrary Assay Design Center (Roche applied science) and their sequences are reported in Table 1. Amplification program included an initial denaturation at 94 °C for 5 min followed by 45 cycles consisting of denaturation at 94

°C for 10 s, annealing at 60 °C for 20 s and extension at 72 °C for 15 s. Data were collected using the Light Cycler 480 software (Platform AVB, iSm2, Marseille, France). Target mRNA levels were normalized to GAPDH mRNA level (house-keeping gene). The relative quantification of target mRNA levels was performed using the comparative ΔΔCt method (Livak and Schmittgen, 2001).

Quantification of the production of nitric oxide (NO).

Nitric oxide production by Caco-2 cells was assessed indirectly by measuring nitrite concentration using the Griess reaction, as previously explained (Maresca et al., 2005; Razafimanjato et al., 2011). Briefly, 100 µl aliquots of culture supernatants collected apically or basolaterally from Caco-2 inserts were incubated with 100 µl of Griess reagent (1 % sulphanilamide, 0.1 % N-(1-naphthyl)ethylenediamine dihydrochloride and 5 % phosphoric acid) at room temperature for 10 min. OD was then measured at 570 nm and the corresponding nitrite concentration was determined using a sodium nitrite standard curve.

Quantification of iNOS protein.

The content of iNOS protein was measured using western-blot analysis. Cells grown on 1 cm^2 inserts were washed with cold PBS and solubilized on ice with 100 µl of lysis buffer (1 % Triton X-100 in cold PBS) containing protease inhibitor cocktail (Sigma Aldrich). Protein concentrations were determined by the Bradford Reagent (Sigma Aldrich) assay as per manufacturer's instructions. Twenty-five microlitres of 5X Laemmlli sample buffer were added and samples boiled for 10 min. Samples containing 50 µg of protein were separated on 4-12 % precast SDS-PAGE gels (Thermo Fisher) before transferring to a nitrocellulose membrane using Fast Blot

system (Thermo Fisher). The membrane was incubated for 1 h at room temperature in PBS containing 5 % non-fat dried milk, washed with PBS and incubated for 1 h with the appropriate primary antibody diluted in PBS as per manufacturer's suggestions (i.e. 1:100 dilution). Rabbit polyclonal antibodies against human iNOS (sc-651) and actin (A-2066) were from Santa Cruz and Sigma Aldrich, respectively. Membranes were washed three times with PBS and incubated for 1 h with alkaline phosphatase-conjugated goat anti-rabbit immunoglobulin G secondary antibody (Jackson Immunoresearch). Membranes were washed extensively and developed with alkaline phosphatase substrate (NBT/BCIP) (Pierce). Band densities were measured using ImageJ software, iNOS levels being normalized to actin staining. In addition to western-blot analysis, iNOS protein content was also evaluated using immunofluorescence microscopy. Caco-2 inserts were washed with cold PBS and fixed with 4 % PFA during 60 min at room temperature. After three washes with PBS, cells were permeabilized and blocked for 30 min in PBS supplemented with Triton X100 (0.1 % final) and BSA (5 % final). After being washed with PBS, cells were labeled with primary antibodies directed against iNOS (sc-651 from Santa Cruz, 1:100 dilution in PBS plus 0.5 % BSA and 0.1 % Triton X-100) for 1 h. After three washes with PBS, specific secondary antibody conjugated to AlexaFluor-488 (Invitrogen) was added (1:200 dilution in PBS plus 0.5 % BSA and 0.1 % Triton X-100). Actin was labeled using Phalloidin conjugated to fluoroprobe 547H (from Interchim, 1:50 dilution). After 1h incubation at room temperature, cells were washed six times with PBS, the inserts were cut using a razor blade and were mounted in Vectashield medium, sealed with nail varnish and viewed using similar settings with an epifluorescence microscope (Leitz DMRB microscope (Leïca) equipped with Leïca DFC 450C camera).

Quantification of the proteasome activity.

Proteasome activity was measured using the specific fluorescent substrate Suc-LLVY-AMC (from Merck). Caco-2 cells seeded onto 1 cm^2 inserts were treated with 1, 10 or 100 µM of DON plus or minus cytomix for 12 or 24 h. At the end of the incubation, cells were washed with PBS, scrapped in 500 µl of PBS on ice and centrifuged at 500 g for 5 min. Cells were then lysed 30 min on ice with 100 µl of ice cold lysis buffer containing TrisHCl (20 mM, pH 7.8), EDTA (5 mM), NaCl (150 mM) and Triton X100 (1 % final). Tubes were centrifuged at 13,000 g for 15 min at 4 °C. Finally, proteasome activity was measured by adding 50 µl of cell extracts to 450 µl of lysis buffer containing 70 µM of Suc-LLVY-AMC. Fluorescence (excitation 380 nm / emission 460 nm) was measured initially and after 30 min of incubation at 30 °C using a spectrofluorometer (Fluoromax-4, Horiba Jobin Yvon).

Evaluation of the ubiquitinylation of total cell proteins and iNOS.

The ubiquitinylation of total cell proteins and iNOS was evaluated by immuno-blot using rabbit anti-ubiquitin antibody from Cell Signaling according to manufacturer's instructions. The ubiquitinylation of total cell proteins was studied after separation of Caco-2 proteins (50 µg per line) on 4-12 % precast SDS-PAGE before immuno-blot. To study the specific ubiquitinylation of iNOS, iNOS protein was first immunoprecipitated from Caco-2 cells seeded onto 4.5 cm^2 inserts using anti-iNOS antibody (Santa Cruz, sc-651) and Pierce immunoprecipitation kit (Direct IP kit) according to manufacturer's instructions (Razafimanjato et al., 2010; 2011). Precipitated iNOS protein was then subjected to 4-12 % SDS-PAGE electrophoresis

before immuno-blotting with anti-ubiquitin antibody and quantification of band densities using ImageJ software.

Statistical analysis.

All experiments were conducted in triplicate. t-Test and two way ANOVA analyses were used to address the significant differences between mean values with significance set at $p < 0.05$ (GraphPad ® Prism5 software).

Results

DON increases iNOS mRNA in Caco-2 cells without increasing iNOS protein or NO production.

We first studied the effect of DON on iNOS mRNA in Caco-2 cells by RT-qPCR. We observed that DON caused a time- and dose-dependent increase in iNOS mRNA expression (Figure 1). The time-dependent study (Figure 1A) showed that DON effect (at 10 µM) was biphasic with an initial increase between 3 and 12 h of exposure (3.9 +/- 1.1-fold increase in iNOS mRNA at 12 h) followed by a decrease between 12 and 24 h of exposure, the iNOS mRNA content at 24 h still being superior to control value (2.4 +/- 0.9-fold increase). The dose-dependent study conducted after 12 h of exposure (Figure 1B) showed that dose-effect was also biphasic, with an initial increase between 0.1 and 1 µM (4.6 +/- 1.5-fold increase at 1 µM) followed by a decrease at 10 and 100 µM, the iNOS mRNA contents at these concentrations still being superior to control value (3.7 +/- 1.3 and 2.5 +/- 0.5-fold increase at 10 and 100 µM, respectively). Although our results demonstrated that DON increased iNOS mRNA content, DON effect was weak compared to cytomix. Indeed, whereas maximal DON effect observed was 4.6-fold increase, cytomix caused a much higher

increase in iNOS mRNA, i.e. a 1,092 +/- 255-fold increase (Figure 3). Next, we determined if DON effect on iNOS mRNA was followed by an effect on iNOS protein and NO production (Figure 2). The effect of DON on iNOS protein was evaluated by immuno-blot using cytomix treatment as positive control (Figure 2A). As expected, cytomix induced a strong increase in iNOS protein content. Results also demonstrated that DON, although increasing iNOS mRNA, failed at inducing detectable iNOS protein production. Measurement of the production of NO confirmed that cytomix, but not DON, was able to cause an efficient expression of iNOS protein (Figure 2B). Interestingly and consistently with the literature and our previous studies (Maresca et al., 2005), we found that the induction of iNOS expression by cytomix resulted in an asymmetric NO secretion, the apical nitrite content being superior to the basolateral one (12.2 +/- 1.9 and 2.9 +/- 0.5 µM, respectively) as previously reported (Maresca et al., 2005; Vallance et al., 2002; Witthoft et al., 1998). We studied the effect of DON on cytokine-mediated increase in iNOS mRNA (Figure 3). Results showed that DON did not modify cytomix-mediated iNOS mRNA production, except at 10 µM where a two-fold increase in cytomix effect was observed (i.e. 1,094 +/- 255 and 2.244 +/- 489-fold increase with cytomix or cytomix plus 10 µM of DON, respectively).

DON decreases the amount of iNOS protein and NO production in cytomix-treated IEC cells in the absence of cellular toxicity.

Next, we studied the effect of DON on iNOS protein and NO production induced by cytomix. Surprisingly, and contrarily to mRNA results, we found that DON dose-dependently decreased iNOS protein induction by cytomix (Figures 4 and 5). Immuno-blot analysis showed that half-inhibition was observed at 1 µM of DON (51.5

+/- 12.6 % inhibition), almost total suppression of cytomix effect being observed at 10 and 100 µM of DON (96.9 +/- 8.7 and 98.7 +/- 4.9 % inhibition, respectively) (Figure 4). Evaluation of iNOS protein content by immuno-fluorescence microscopy (Figure 5) and NO measurement (Figure 6) confirmed western-blot analysis. Results showed that DON dose-dependently suppressed both apical and basolateral cytokine-mediated secretion of nitrite with 53.9 +/- 6.9 and 58.4 +/- 8.3 % of inhibition of apical and basolateral nitrite secretion at 1 µM of DON and more than 90 % of inhibition for concentrations superior or equal to 10 µM.

Since DON is known to cause cell toxicity, we wondered if cell viability was affected at concentrations inhibiting cytomix-mediated iNOS induction. Cell toxicity was evaluated using LDH assay after incubation of Caco-2 cells with increasing concentrations of DON for 24 h in the presence or absence of cytomix (Figure 7A). In all conditions, no toxicity was observed at concentrations of DON inferior or equal to 10 µM, cellular toxicity being observed only at 100 µM of DON, in accordance with our previous publication (Maresca et al., 2008). Similarly, measurement of interleukin-8 (IL-8) secretion (Figure 7B) showed that DON decreased IL-8 secretion caused by cytomix only at 100 µM (58.3 +/- 13.7 % inhibition), confirming the absence of general toxicity or protein synthesis inhibition at concentrations inferior or equal to 10 µM.

DON effect on iNOS protein depends on its degradation by the proteasome.

The half-life of iNOS protein depends on both gene expression and proteasome-mediated degradation (Chow et al., 2009; Jin et al., 2009). Since our results proved that inhibition of cytomix-mediated induction of iNOS by DON is not related to gene

expression (Figure 3), we decided to evaluate the involvement of proteasome activity in DON effect. The effect of lactacystin, a known specific inhibitor of proteasome activity, was tested on Caco-2 cells treated with cytomix and DON (Figure 8). Lactacystin was added with DON 6 h after cytomix treatment started since, as described by others (Jin et al., 2009; Qureshi et al., 2012), our preliminary experiments showed that adding lactacystin earlier suppressed cytomix-mediated iNOS induction. Although lactacystin alone did not induce iNOS expression (data not shown), we observed that lactacystin, by limiting its degradation, significantly increased the amount of iNOS protein in cytomix-treated cells (34.9 +/- 12.3 % increase). Immuno-blot analysis demonstrated that lactacystin at least partially prevented the inhibitory effect of DON on iNOS protein (Figure 8A), iNOS protein production being decreased by DON by 98.1 +/- 6.5 and 36.8 +/- 9.4 % in the absence and presence of lactacystin, respectively (Figure 8B). Nitrite measurement confirmed western-blot results with nitrite concentrations being of 12.2 +/- 1.9 ; 1.4 +/- 0.38 and 5.9 +/- 2.1 µM and 2.9 +/- 0.5; 0.35 +/- 0.26 and 1.9 +/- 0.9 µM in the apical and basolateral media of cells treated with cytomix, cytomix plus DON and cytomix plus DON plus lactacystin, respectively. Finally, we tested the effect of DON on iNOS half-life (Figure 9). Caco-2 cells were treated with cytomix for 24 h to induce massive accumulation of iNOS protein. Cells were then treated with DON (10 µM) for 6, 12 or 24 h. Results showed that DON accelerated the degradation of already produced iNOS compared to untreated cells and that lactacystin prevented such degradation.

DON increases the ubiquitinylation of iNOS.

The degradation of iNOS protein caused by DON could rely either on increased activity of proteasome and / or increased ubiquitinylation of iNOS. We first tested the effect of DON plus or minus cytomix on proteasome activity using a specific fluorescent substrate (Suc-LLVY-AMC) (Figure 10). Results showed that exposure of Caco-2 cells to 1 µM of DON for 12 and 24 h increased proteasome activity particularly in the presence of cytomix (18 and 32 % increase, respectively, compared to control). At 10 µM, DON induced a weak inhibition of proteasome activity in the presence or absence of cytomix (ranging from 1 to 15 % of inhibition). Only 100 µM of DON significantly inhibited proteasome activity (i.e. around 50 % of inhibition after 24 h exposure) in accordance with its demonstrated toxicity at this concentration (Figure 7). Next, we looked at the effect of DON on the ubiquitinylation of proteins (Figure 11). Evaluation of the effect of DON on the ubiquitinylation of total cell proteins showed that DON did not induce major changes in the ubiquitinylation profile of Caco-2 cell extract, except a band with an apparent molecular weight around 40 kDa only present in DON and cytomix-treated cells (Figure 11A). At present, the nature of this protein or its role in DON effect remain unknown. Importantly, analysis conducted on immuno-precipitated iNOS showed that DON caused a significant increase in ubiquitinylation of iNOS protein (295 +/- 21 % of control value) (Figure 11B).

The degradation of iNOS induced by DON relies on the activation of PKR, MAP kinases and NFκB.

Finally, we evaluated the role played by signal pathways in the effect of DON on iNOS degradation. Inhibitors of the protein kinase R (PKR) (adenine, 2 mM), the MAP

kinases ERK1/2 (PD 98059, 50 µM) and p38 (SB 203580, 20 µM) or of the NFκB pathway (PDTC, 100 µM) were tested and compared to lactacystin (25 µM). Preliminary experiments showed that adding the inhibitors in the same time than cytomix inhibited iNOS induction in accordance with the role played by these signal pathways in iNOS mRNA production and stabilization (Maresca et al., 2005) (data not shown). For this reason, inhibitors were added with DON 6 h after that cytomix treatment started (Figure 12). Results showed that all the inhibitors tested partially prevented DON mediated suppression of iNOS induction by cytomix, lactacystin being the more active. Efficiency of the inhibitors to prevent DON-mediated degradation of already produced iNOS protein were also tested (Figure 13). Caco-2 cells were treated for 24 h with cytomix to induce iNOS protein accumulation. Cells were then treated for 24 h with DON plus or minus inhibitors. Results confirmed that all the inhibitors tested partially stopped DON-mediated degradation of iNOS protein, lactacystin being again the more efficient.

Discussion

Exposure to DON has deleterious effects on intestinal functions, including gut immunity (Bouhet and Oswald, 2005; Bracarense et al., 2012; Ghareeb et al., 2014; Maresca, 2013; Pinton and Oswald, 2014). Accordingly, DON is known to increase the susceptibility of animals to intestinal infection by bacteria and viruses (Antonissen et al., 2014; Maresca, 2013). Although a compromised intestinal barrier function and an increase in bacterial translocation caused by DON may explained such phenomena (particularly in the case of bacterial infection), an additional specific

inhibition of the production of epithelial antimicrobial factors, including NO, could not be ruled-out.

Literature on the effects of DON on the expression of iNOS by the intestinal epithelium is scarce, only a pioneer study from Gajęcki's group in 2013 showing that exposure to DON modulates iNOS mRNA levels in the intestine of pigs (Gajęcka et al., 2013). In the present study, we aimed to evaluate the effect of DON on intestinal iNOS induction in term of mRNA, protein and NO production. Results showed that, like in pig duodenum (Gajęcka et al., 2013), DON increases the level of iNOS mRNA in human IEC, such increase being low compared to the one mediated by a cocktail of proinflammatory cytokines (cytomix). Since the production and stability of iNOS mRNA depend on signal pathways including NFκB and MAP kinases (Maresca et al., 2005) it is not surprising that DON and cytomix, that have in common to activate these signal pathways (Pestka, 2010, Maresca, 2013), increase iNOS mRNA content. However, the increase in iNOS mRNA caused by DON in human IEC was not followed by an increase in iNOS protein level or NO production. Indeed, we observed that DON decreased the level of iNOS protein and NO production in cytomix-treated cells with half inhibition at 1 μM and full inhibition at concentrations superior or equal to 10 μM of toxin.

The decrease in iNOS protein level caused by DON could either rely on a decrease in iNOS protein production and / or an increase in iNOS protein degradation by the proteasome. Proteasome plays dual roles in iNOS induction. First, proteasome activity is involved in the cytokine-mediated activation of NFκB through the

degradation of the NFκB inhibitor (IkB), allowing the expression of iNOS gene and the production of iNOS mRNA (Maresca et al., 2008). But in the mean time, proteasome activity is also responsible for the degradation of produced iNOS protein (Chow et al., 2009; Jin et al., 2009). Our results proved that DON does not decrease the production of iNOS mRNA. Instead, we found that DON accelerates iNOS degradation, decreasing the half-life of iNOS proteins already present in human IEC and that lactacystin, a specific proteasome inhibitor prevents such effect. Taken together, thus it seems highly unlikely that the effect of DON on iNOS protein is due to alteration of protein production but rather relies on iNOS degradation by the proteasome. Prior to be degraded by the proteasome, target proteins have to be tagged with ubiquitin, a reaction called ubiquitinylation that involves ubiquitin ligases (Inobe and Matouschek, 2014). Accordingly, our results showed that DON increases the specific ubiquitinylation of iNOS protein. The mechanism involved in the increased ubiquitinylation of iNOS caused by DON is still uncharacterized at present. It could rely either on iNOS misfolding or activation of ubiquitin ligases (Nogueira da Costa et al., 2011; Osman et al., 2010). The use of specific inhibitors of signal pathways demonstrated that, in addition and prior to proteasome action, DON-induced degradation of iNOS relies on the activation by the toxin of the PKR, the MAP kinases (p38 and ERK1/2) and of NFκB, such signal pathways being known to be associated to DON effects in various animals and cell models (Arunachalam and Doohan, 2013; Maresca, 2013; Pestka, 2010).

The proteasome-dependent degradation of iNOS protein caused by DON may explain why although DON increases iNOS mRNA in human IEC, it fails at causing iNOS protein expression and NO production. Interestingly, an inhibition by DON of

iNOS was also reported in immune cells. A decrease in LPS-mediated NO production was thus observed in macrophages and microgial cells exposed to DON (Ji et al., 1998; Razafimanjato et al., 2011; Sugiyama et al., 2010; 2011). But contrarily to the results obtained in the present study, suppression of NO production in these immune cells happens at concentrations of DON associated to cell toxicity. Accordingly, a decrease in the LPS-mediated production of iNOS mRNA was observed in macrophages exposed to DON (Sugiyama et al., 2010). This suggests that DON could use different mechanisms to inhibit a similar target (i.e. iNOS) in immune cells and IEC, another possibility being that the proteasome-mediated degradation also happens in immune cells but is masked by cell toxicity in that case.

Since iNOS suppression by DON in IEC is observed at low concentrations (as low as 1 µM), we believe that such effect may happens in humans exposed to contaminated food. Such observations should alert food agencies and potentially lead to the reevaluation of the actual PMTDI for DON. Indeed, our work shows that low concentrations of DON already known to cause the secretion of cytokines and intestinal inflammation (Maresca et al., 2008) are in the mean time able to suppress epithelial iNOS induction and NO production. This leads to a counterintuitive situation in which the gut mucosa is inflamed but unarmed against microbial invaders, in accordance with the in vivo observations showing that exposure of animals to DON leads to intestinal inflammation and a parallel increase in the susceptibility to intestinal infection.

Funding information:

This work was supported by the Centre National de la Recherche Scientifique and the Ministère de l'Enseignement Supérieur et de la Recherche Scientifique.

Acknowledgments: We would like to thank Dr Elise Courvoisier-Dezord in charge of the maintenance of the qPCR system at the AVB platform (iSm2, Marseille) and Dr Pierre Rousselot-Pailley for his assistance with the fluorometer.

References.

Alam, M. S., Akaike, T., Okamoto, S., Kubota, T., Yoshitake, J., Sawa, T., Miyamoto, Y., Tamura, F., and Maeda, H. (2002). Role of nitric oxide in host defense in murine salmonellosis as a function of its antibacterial and antiapoptotic activities. *Infect. Immun.* **70**, 3130–3142.

Antonissen, G., Martel, A., Pasmans, F., Ducatelle, R., Verbrugghe, E., Vandenbroucke, V., Li, S., Haesebrouck, F., Van Immerseel, F., and Croubels, S. (2014). The impact of Fusarium mycotoxins on human and animal host susceptibility to infectious diseases. *Toxins (Basel)*. **6**, 430-452.

Arunachalam, C., and Doohan, F. M. (2013). Trichothecene toxicity in eukaryotes: cellular and molecular mechanisms in plants and animals. *Toxicol. Lett.* **217**, 149-158.

Awad, W., Ghareeb, K., Böhm, J., and Zentek, J. (2013). The toxicological impacts of the Fusarium mycotoxin, deoxynivalenol, in poultry flocks with special reference to immunotoxicity. *Toxins (Basel).* **5**, 912-925.

Bracarense, A. P., Lucioli, J., Grenier, B., Drociunas Pacheco, G., Moll, W. D., Schatzmayr, G., and Oswald, I. P. (2012). Chronic ingestion of deoxynivalenol and fumonisin, alone or in interaction, induces morphological and immunological changes in the intestine of piglets. *Br. J. Nutr.* **107**, 1776-1786.

Bouhet, S., and Oswald, I. P. (2005). The effects of mycotoxins, fungal food contaminants, on the intestinal epithelial cell-derived innate immune response. *Vet. Immunol. Immunopathol*. **108**, 199-209.

Cano, P. M., Seeboth, J., Meurens, F., Cognie, J., Abrami, R., Oswald, I. P., and Guzylack-Piriou, L. (2013). Deoxynivalenol as a new factor in the persistence of intestinal inflammatory diseases: an emerging hypothesis through possible modulation of Th17-mediated response. *PLoS One*. **8**, e53647.

Chow, J. M., Lin, H. Y., Shen, S. C., Wu, M. S., Lin, C. W., Chiu, W. T., Lin, C. H., and Chen, Y. C. (2009). Zinc protoporphyrin inhibition of lipopolysaccharide-, lipoteichoic acid-, and peptidoglycan-induced nitric oxide production through stimulating iNOS protein ubiquitination. *Toxicol. Appl. Pharmacol.* **237**, 357-365.

Elliott, S. N., and Wallace, J. L. (1998). Nitric oxide: a regulator of mucosal defense and injury. *J. Gastroenterol*. **33**, 792-803.

Gajęcka, M., Stopa, E., Tarasiuk, M., Zielonka, L., and Gajęcki, M. (2013). The expression of type-1 and type-2 nitric oxide synthase in selected tissues of the gastrointestinal tract during mixed mycotoxicosis. *Toxins (Basel).* **5**, 2281-2292.

Gerez, J. R., Pinton, P., Callu, P., Grosjean, F., Oswald, I. P., and Bracarense, A. P. (2014). Deoxynivalenol alone or in combination with nivalenol and zearalenone induce systemic histological changes in pigs. *Exp. Toxicol. Pathol*. pii: S0940-2993(14)00143-2. doi: 10.1016/j.etp.2014.10.001.

Ghareeb, K., Awad, W. A., Böhm, J., and Zebeli, Q. (2014). Impacts of the feed contaminant deoxynivalenol on the intestine of monogastric animals: poultry and swine. *J. Appl. Toxicol.* Advance Access published October 28, 2014. doi: 10.1002/jat.3083.

Inobe, T., and Matouschek, A. (2014). Paradigms of protein degradation by the proteasome. *Curr. Opin. Struct. Biol*. **24**, 156-164.

Ji, G. E., Park, S. Y., Wong, S. S., and Pestka, J. J. (1998). Modulation of nitric oxide, hydrogen peroxide and cytokine production in a clonal macrophage model by the trichothecene vomitoxin (deoxynivalenol). *Toxicology*. **125**, 203–214.

Jin, H. K., Ahn, S. H., Yoon, J. W., Park, J. W., Lee, E. K., Yoo, J. S., Lee, J. C., Choi, W. S., and Han, J. W. (2009). Rapamycin down-regulates inducible nitric oxide synthase by inducing proteasomal degradation. *Biol. Pharm. Bull.* **32**, 988-992.

Kagnoff, M. F. (2014). The intestinal epithelium is an integral component of a communications network. *J. Clin. Invest.* **124**, 2841-2843.

Livak, K. J., and Schmittgen, T. D.(2001). Analysis of relative gene expression data using real-time quantitative PCR and the 2(-Delta Delta C(T)) Method. *Methods.* **25**, 402-408.

Mattsson, J. L. (2007). Mixtures in the real world: the importance of plant self-defense toxicants, mycotoxins, and the human diet. *Toxicol. Appl. Pharmacol.* **223**, 125–132.

Maresca, M., Miller, D., Quitard, S., Dean, P., and Kenny, B. (2005). Enteropathogenic Escherichia coli (EPEC) effector-mediated suppression of antimicrobial nitric oxide production in a small intestinal epithelial model system. *Cell. Microbiol.* **7**, 1749-1762.

Maresca, M., Yahi, N., Younès-Sakr, L., Boyron, M., Caporiccio, B., and Fantini, J. (2008). Both direct and indirect effects account for the pro-inflammatory activity of enteropathogenic mycotoxins on the human intestinal epithelium: stimulation of interleukin-8 secretion, potentiation of interleukin-1beta effect and increase in the transepithelial passage of commensal bacteria. *Toxicol. Appl. Pharmacol.* **228**, 84-92.

Maresca, M., and Fantini, J. (2010). Some food-associated mycotoxins as potential risk factors in humans predisposed to chronic intestinal inflammatory diseases. *Toxicon.* **56**, 282-294.

Maresca, M. (2013). From the gut to the brain: journey and pathophysiological effects of the food-associated trichothecene mycotoxin deoxynivalenol. *Toxins (Basel).* **5**, 784-820.

Moens, E., and Veldhoen, M. (2012). Epithelial barrier biology: good fences make good neighbours. *Immunology.* **135**, 1-8.

Nogueira da Costa, A., Mijal, R. S., Keen, J. N., Findlay, J. B., and Wild, C. P. (2011). Proteomic analysis of the effects of the immunomodulatory mycotoxin deoxynivalenol. *Proteomics.* **11**, 1903-1914.

Osman, A. M., Pennings, J. L., Blokland, M., Peijnenburg, A., and van Loveren, H. (2010). Protein expression profiling of mouse thymoma cells upon exposure to the trichothecene deoxynivalenol (DON): implications for its mechanism of action. *J. Immunotoxicol.* **7**, 147-156.

Pestka, J. J. (2010). Deoxynivalenol: Mechanisms of action, human exposure, and toxicological relevance. *Arch. Toxicol.* **84**, 663–679.

Pinton, P., Oswald, I. P. (2014). Effect of deoxynivalenol and other Type B trichothecenes on the intestine: a review. *Toxins (Basel).* **6**, 1615-1643.

Qureshi, A. A., Guan, X. Q., Reis, J. C., Papasian, C. J., Jabre, S., Morrison, D. C., and Qureshi, N. (2012). Inhibition of nitric oxide and inflammatory cytokines in LPS-stimulated murine macrophages by resveratrol, a potent proteasome inhibitor. *Lipids Health Dis.* **11**, 76.

Razafimanjato, H., Garmy, N., Guo, X. J., Varini, K., Di Scala, C., Di Pasquale, E., Taïeb, N., and Maresca, M. (2010). The food-associated fungal neurotoxin ochratoxin A inhibits the absorption of glutamate by astrocytes through a decrease in cell

surface expression of the excitatory amino-acid transporters GLAST and GLT-1. *Neurotoxicology.* **31**, 475-484.

Razafimanjato, H., Benzaria, A., Taïeb, N., Guo, X. J., Vidal, N., Di Scala, C., Varini, K., and Maresca, M. (2011). The ribotoxin deoxynivalenol affects the viability and functions of glial cells. *Glia.* **59**, 1672-1683.

Saint-Cyr, M. J., Perrin-Guyomard, A., Houée, P., Rolland, J. G., and Laurentie, M. (2013). Evaluation of an oral subchronic exposure of deoxynivalenol on the composition of human gut microbiota in a model of human microbiota-associated rats. *PLoS One*. **8**, e80578.

Salzman, A. L., Eaves-Pyles, T., Linn, S. C., Denenberg, A. G., and Szabo, C. (1998). Bacterial induction of inducible nitric oxide synthase in cultured human intestinal epithelial cells. *Gastroenterology.* **114**, 93–102.

Santaolalla, R., and Abreu, M. T. (2012). Innate immunity in the small intestine. *Curr. Opin. Gastroenterol.* **28**, 124-129.

Sugiyama, K., Muroi, M., Tanamoto, K., Nishijima, M., and Sugita-Konishi, Y. (2010). Deoxynivalenol and nivalenol inhibit lipopolysaccharideinduced nitric oxide production by mouse macrophage cells. *Toxicol. Lett.* **192**, 150–154.

Sugiyama, K., Kawakami, H., Kamata, Y., and Sugita-Konishi, Y. (2011). Effect of a combination of deoxynivalenol and nivalenol on lipopolisaccharide-induced nitric oxide production by mouse macrophages. *Mycotoxin Res.* **27**, 57-62

Vallance, B. A., Deng, W., De Grado, M., Chan, C., Jacobson, K., and Finlay, B. B. (2002). Modulation of inducible nitric oxide synthase expression by the attaching and effacing bacterial pathogen Citrobacter rodentium in infected mice. *Infect. Immun.* **70**, 6424–6435.

Witthoft, T., Eckmann, L., Kim, J. M., and Kagnoff, M. F. (1998). Enteroinvasive bacteria directly activate expression of iNOS and NO production in human colon epithelial cells. *Am. J. Physiol.* **275**, G564–G571.

Wu, F., Groopman, J. D., and Pestka, J. J. (2014a). Public health impacts of foodborne mycotoxins. *Annu. Rev. Food Sci. Technol.* **5**, 351-372.

Wu, W., Zhou, H. R., Bursian, S. J., Pan, X., Link, J. E., Berthiller, F., Adam, G., Krantis, A., Durst, T., and Pestka, J. J. (2014b). Comparison of anorectic and emetic potencies of deoxynivalenol (vomitoxin) to the plant metabolite deoxynivalenol-3-glucoside and synthetic deoxynivalenol derivatives EN139528 and EN139544. *Toxicol. Sci*. **142**, 167-181.

Wu, W., He, K., Zhou, H. R., Berthiller, F., Adam, G., Sugita-Konishi, Y., Watanabe, M., Krantis, A., Durst, T., Zhang, H., and Pestka, J. J. (2014c). Effects of oral exposure to naturally-occurring and synthetic deoxynivalenol congeners on

proinflammatory cytokine and chemokine mRNA expression in the mouse. *Toxicol. Appl. Pharmacol*. **278**, 107-115.

Figure legend.

Figure 1 : DON induces the production of iNOS mRNA in human IEC.

Caco-2 cells seeded onto 1 cm^2 inserts were apically treated with 10 µM of DON for 3, 6, 12 or 24 h (**A**) or for 12 h with increasing concentration of DON (**B**). At the end of the incubation, mRNA were extracted and quantified, as explained in Materials and Methods. iNOS mRNA were normalized using GAPDH mRNA. Results were expressed as fold increase in iNOS mRNA content compared to untreated cells (means +/- SD, with * $p < 0.05$ and ** $p < 0.01$ (n = 3)).

Figure 2 : DON does not induce iNOS protein or NO secretion.

Caco-2 cells seeded onto 1 cm^2 inserts were apically treated for 24 h with increasing concentrations of DON. At the end of the incubation, iNOS protein (**A**) and NO production (**B**) were measured as explained in Materials and Methods. Caco-2 cells basolaterally treated with cytomix were used as positive control of iNOS induction. Western-blot showed in (**A**) is representative of three independent experiments. Results showed in (**B**) were expressed as mean +/- SD, with * $p < 0.01$ (n = 3).

Figure 3 : DON does not affect cytomix effect on iNOS mRNA.

Caco-2 cells seeded onto 1 cm^2 inserts were left untreated or were basolaterally treated with cytomix and apically with increasing concentrations of DON for 12 h. At the end of the incubation, mRNA were extracted and quantified, as explained in

Materials and Methods. iNOS mRNA were normalized using GAPDH mRNA. Results were expressed as fold increase in iNOS mRNA content compared to untreated cells. Bars without a common letter differ by at least $p < 0.05$.

Figure 4 : DON decreases iNOS protein in cytomix-treated human IEC.

Caco-2 cells seeded onto 1 cm^2 inserts were left untreated or were basolaterally treated with cytomix and apically with increasing concentrations of DON for 24 h. At the end of the incubation, iNOS protein content was quantified by immuno-blot as explained in Material and Methods. Western-blot showed in (**A**) is representative of three independent experiments. The intensities of bands were measured using ImageJ software. iNOS protein staining was normalized to actin signal. Results in (**B**) were expressed as percentage of control iNOS signal obtained with cytomix treated cells (means +/- SD, with * $p < 0.05$ and ** $p < 0.01$ (n = 3)).

Figure 5 : Fluorescent microscopy confirms the decrease in iNOS protein caused by DON.

Caco-2 cells seeded onto 1 cm^2 inserts were left untreated or were basolaterally treated with cytomix and apically with increasing concentrations of DON for 24 h. At the end of the incubation, iNOS protein content was quantified by immuno-fluorescence analysis as explained in Material and Methods. Images A, C, E, G, I, K correspond to iNOS staining (colored in green). Images B, D, F, H, J, L to actin staining (colored in red). Conditions were : A, B = untreated cells; C, D = cytomix-treated cells ; E, F = cytomix plus DON 0.1 µM ; G, H = cytomix plus DON 1 µM ; I, J

= cytomix plus DON 10 µM ; K, L = cytomix plus DON 100 µM. Color image is available in the online version of the article.

Figure 6 : DON inhibits cytomix-mediated NO production.

Caco-2 cells seeded onto 1 cm^2 inserts were left untreated or were basolaterally treated with cytomix and apically with increasing concentrations of DON for 24 h. At the end of the incubation, apical and basolateral NO production were measured as explained in Materials and Methods. Results were expressed as mean +/- SD, with * $p < 0.05$ and ** $p < 0.01$ (n = 3).

Figure 7 : Only high concentrations of DON cause cell toxicity.

A- Caco-2 cells seeded onto 1 cm^2 inserts were apically treated with increasing concentrations of DON for 24 h in the presence (black columns) or absence (grey columns) of cytomix added basolaterally. At the end of the incubation, LDH release was measured as explained in Materials and Methods. Results were expressed as mean +/- SD, with * $p < 0.01$ (n = 3). **B**- Caco-2 cells were treated with cytomix (added basolaterally) or cytomix and increasing concentrations of DON (added apically) for 24 h before measurement of basolateral IL-8 secretion as indicated in Materials and Methods. Results were expressed as mean +/- SD. Bars without a common letter differ by at least $p < 0.05$.

Figure 8 : Proteasome inhibition reverses DON effect on iNOS protein.

Caco-2 cells seeded onto 1 cm^2 inserts were basolaterally treated with cytomix. 6 h after cytomix treatment started, increasing concentrations of DON were apically added in the presence or absence of lactacystin (25 µM, both apical and basolateral), the incubation being prolongated for 18 h. iNOS protein content was then evaluated using immuno-blot. Western-blot showed in (**A**) is representative of three independent experiments. The intensities of bands were measured using ImageJ software. iNOS protein staining was normalized to actin signal. Results in (**B**) were expressed as percentage of control iNOS signal obtained with cytomix-treated cells. Bars without a common letter differ by at least $p < 0.05$ (n = 3).

Figure 9 : Proteasome inhibition prevents DON-mediated iNOS degradation.

Caco-2 cells seeded onto 1 cm^2 inserts were basolaterally treated with cytomix for 24 h to induce maximal iNOS protein accumulation. Cells were then washed and left untreated or treated with DON (10 µM, apical) for 6, 12 or 24 h in the presence or absence of lactacystin (25 µM, both apical and basolateral). At the end of the incubation, levels of iNOS protein were evaluated using immuno-blot. Western-blot showed in (**A**) is representative of three independent experiments. The intensities of bands were measured using ImageJ software. iNOS protein staining was normalized to actin signals. Results in (**B**) were expressed as percentage of control iNOS signal obtained with cytomix-treated cells. Bars without a common letter differ by at least $p < 0.05$ (n = 3).

Figure 10 : Effect of DON on proteasome activity.

Caco-2 cells seeded onto 1 cm^2 inserts were treated with DON (1, 10 or 100 µM, apical) in the presence (black columns) or absence (grey columns) of cytomix (basolateral) for 12 h (**A**) or 24 h (**B**). At the end of the incubation, proteasome activity (expressed as relative fluorescence unit (RFU)) was measured as explained in Materials and Methods, lactacystin (25 µM) being used as positive control of inhibition. Results were expressed as mean +/- SD, with * p at least < 0.05 (n = 3).

Figure 11 : DON-induced degradation of iNOS relies on an increase in its ubiquitinylation.

Caco-2 cells seeded onto 4.5 cm^2 inserts were treated for 24 h with cytomix (basolateral), DON (10 µM, apical) and / or lactacystin (25 µM, both apical and basolateral). At the end of the incubation, ubiquitinylation of total cell proteins (**A**) or immuno-precipitate iNOS protein (**B**) was measured as explained in Materials and Methods. Results in (**B**) were expressed as percentage of control iNOS or Ub signals obtained with cytomix-treated cells (means +/- SD, with * $p < 0.05$ and ** $p < 0.01$ (n = 3)).

Figure 12 : DON-induced decrease in iNOS protein content depends on PKR, MAP kinases and NFκB.

Caco-2 cells seeded onto 1 cm^2 inserts were basolaterally treated with cytomix. 6 h after cytomix treatment started, DON was apically added in the presence or absence of inhibitors of signal pathways (added both apically and basolaterally) and incubation was prolongated for 18 h. Control without inhibitors received only vehicle (DMSO, 0.1 %). Inhibitors tested were inhibitor of the protein kinase R (PKR) (**Ad**:

adenine, 2 mM), of the MAP kinases ERK1/2 (**PD**: PD 98059, 50 µM) and p38 (**SB**: SB 203580, 20 µM) or of NFκB (**PDTC**, 100 µM). Lactacystin (**LACTA**, 25 µM) was used for comparison. iNOS induction was then evaluated using immuno-blot. Western-blot showed in (**A**) is representative of three independent experiments. The intensities of bands were measured using ImageJ software. iNOS protein staining was normalized to actin signal. Results in (**B**) were expressed as percentage of control iNOS signal obtained with cytomix-treated cells receiving neither DON, nor inhibitors. Bars without a common letter differ by at least $p < 0.05$ (n = 3).

Figure 13 : DON-induced degradation of iNOS protein relies on PKR, MAP kinases and NFκB.

Caco-2 cells seeded onto 1 cm^2 inserts were basolaterally treated with cytomix for 24 h to cause iNOS protein accumulation. DON was then apically added in the presence or absence of inhibitors of signal pathways (added both apically and basolaterally) and the cells were incubated for 24 h. Control without inhibitors received only vehicle (DMSO, 0.1 %). Inhibitors tested were inhibitor of the protein kinase R (PKR) (**Ad**: adenine, 2 mM), of the MAP kinases ERK1/2 (**PD**: PD 98059, 50 µM) and p38 (**SB**: SB 203580, 20 µM) or of NFκB (**PDTC**, 100 µM). Lactacystin (**LACTA**, 25 µM) was used for comparison. iNOS protein content was then evaluated using immuno-blot. Western-blot showed in (**A**) is representative of three independent experiments. The intensities of bands were measured using ImageJ software. iNOS protein staining was normalized to actin signal. Results in (**B**) were expressed as percentage of control iNOS signal obtained with cytomix-treated cells receiving neither DON, nor inhibitors. Bars without a common letter differ by at least $p < 0.05$ (n = 3).

Table 1: Sequences of primers used in this study.

Gene	Accession	Description	Amplicon	Primers	Length	Tm	%GC
GAPDH	NM_002046.3	Glyceraldehyde-3-phosphate dehydrogenase	119 nt	gagtccactggcgtcttcac	20	60	60
				ttcacacccatgacgaacat	20	59	45
iNOS	NM_000625.4	Nitric oxide synthase 2	70 nt	accagtacgtttggcaatgg	20	60	50
				tcagcatgaagagcgatttct	21	60	43

Figure 1

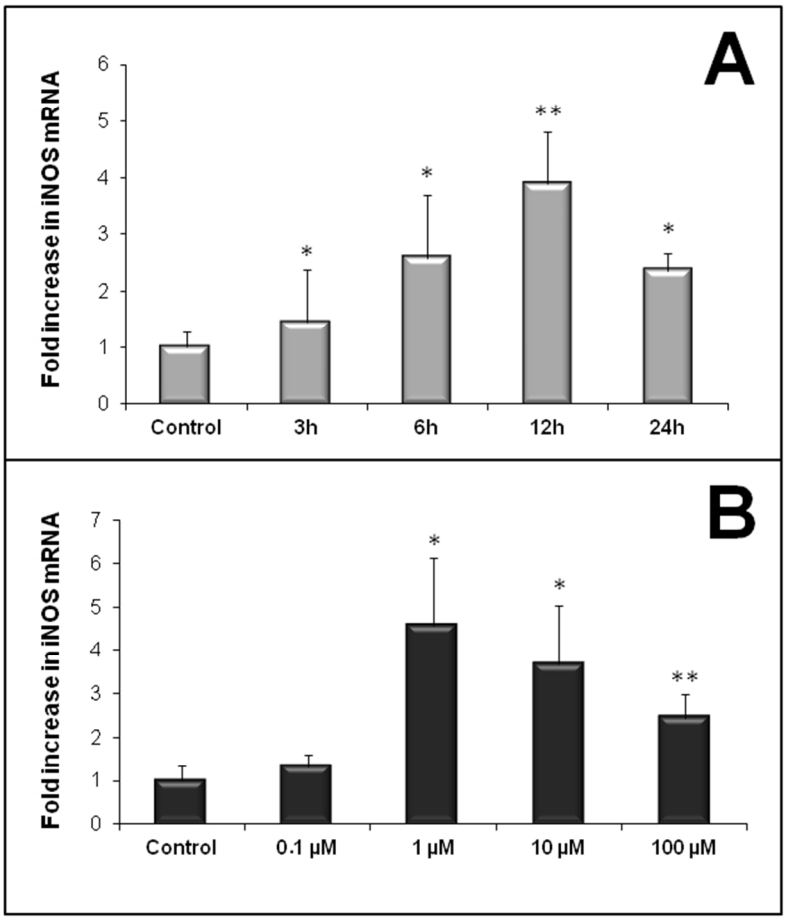

190x254mm (96 x 96 DPI)

Figure 2

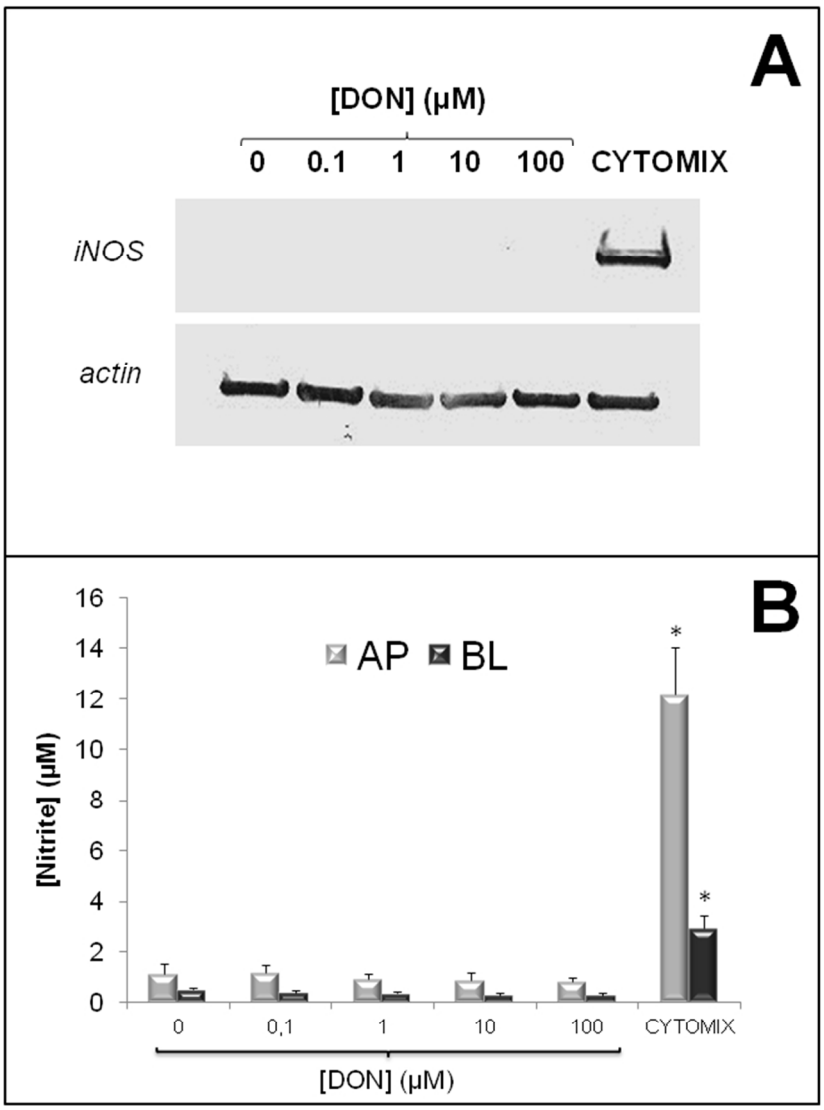

190x254mm (96 x 96 DPI)

Figure 3

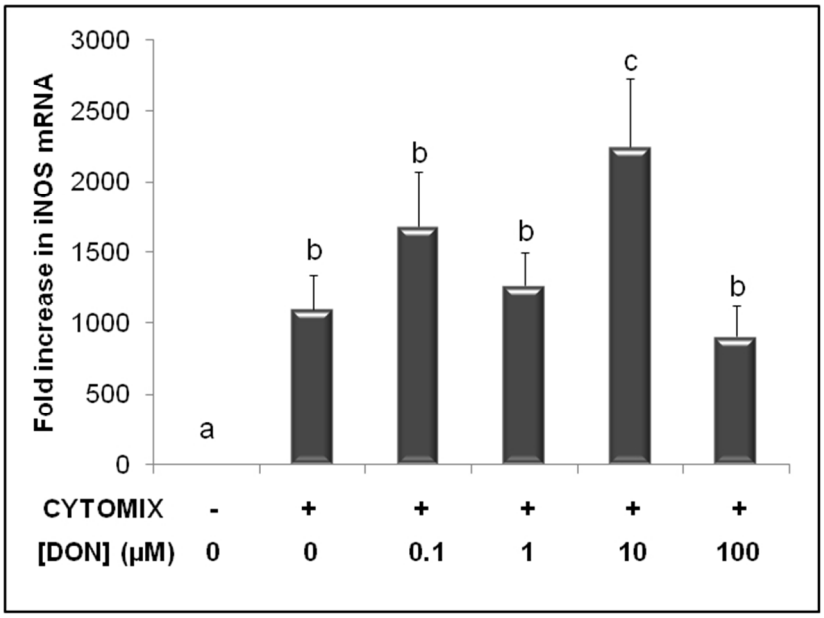

190x254mm (96 x 96 DPI)

Figure 4

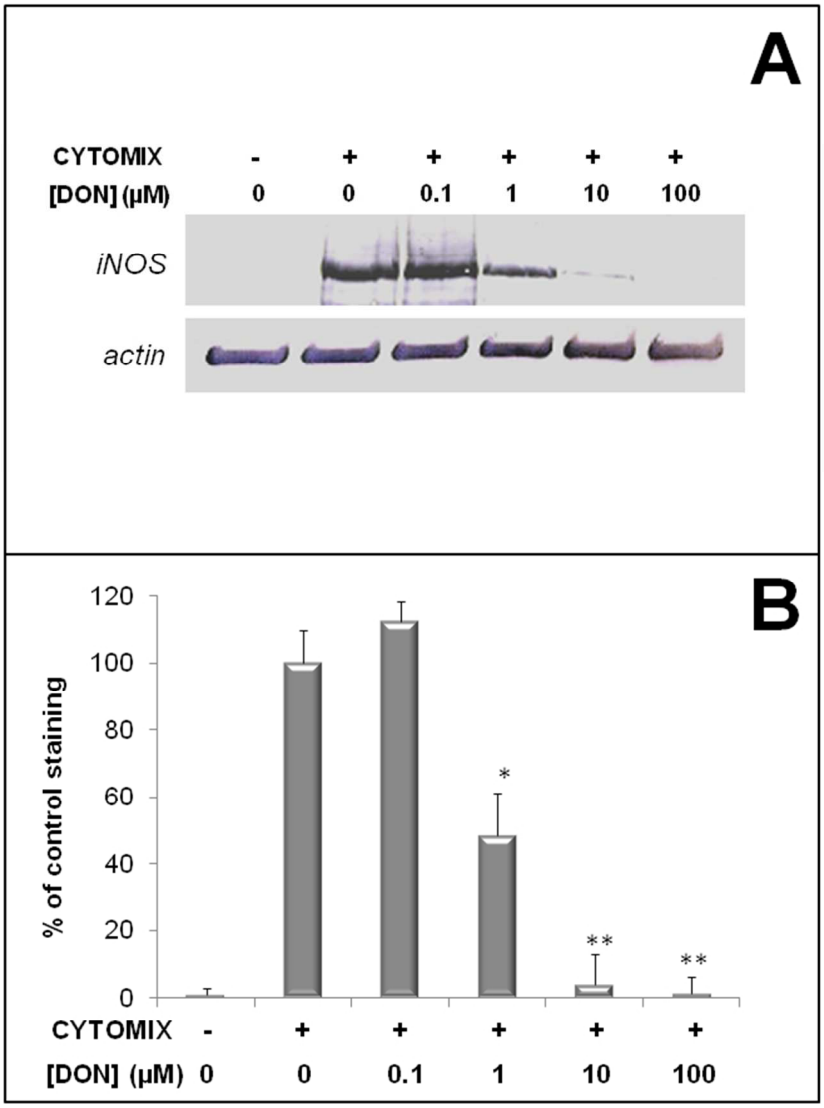

190x254mm (96 x 96 DPI)

Figure 5

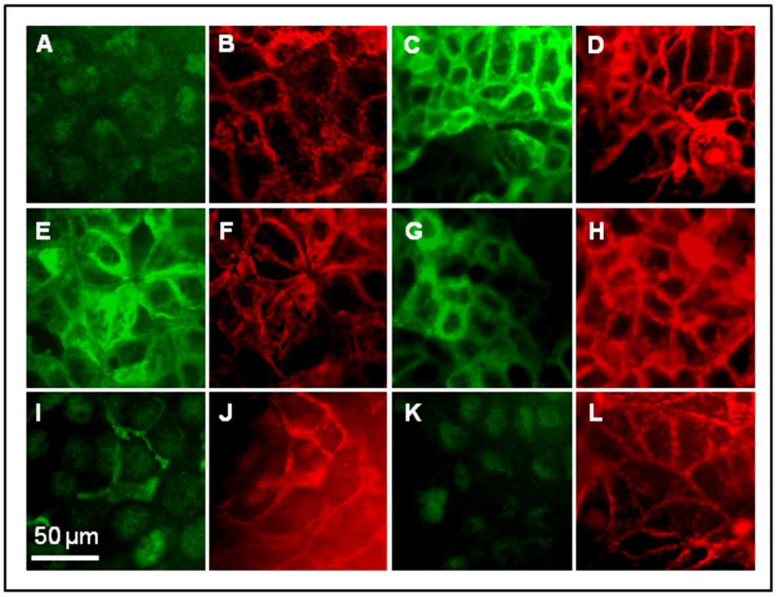

190x254mm (96 x 96 DPI)

Figure 6

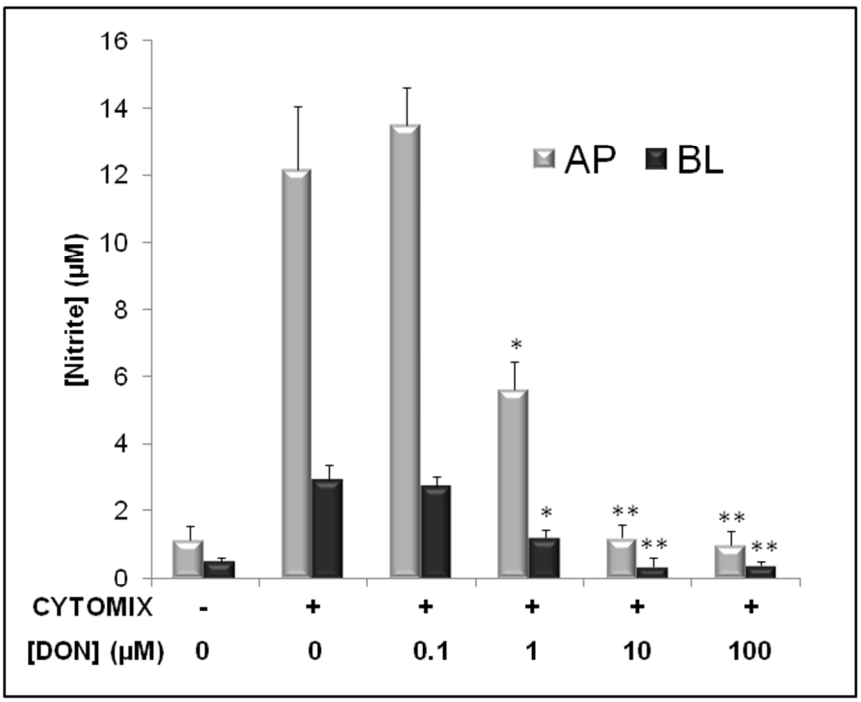

190x254mm (96 x 96 DPI)

Figure 7

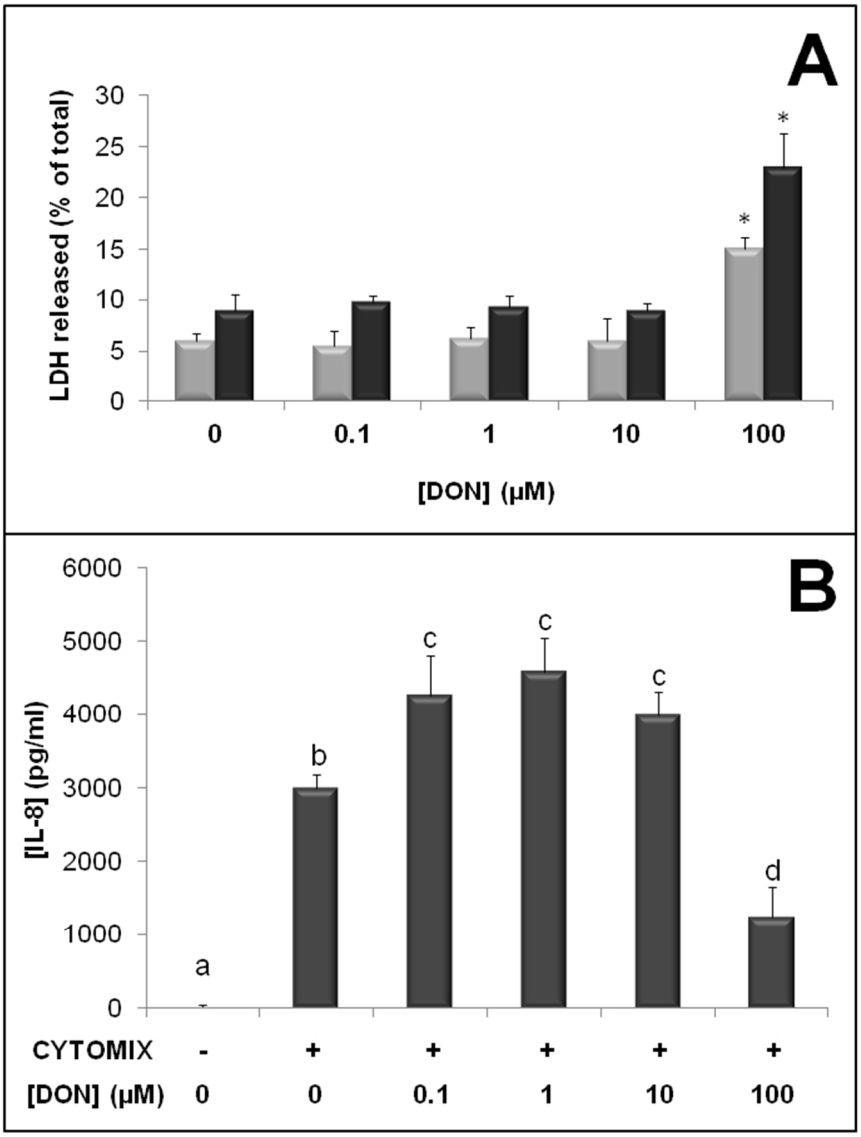

190x254mm (96 x 96 DPI)

Figure 8

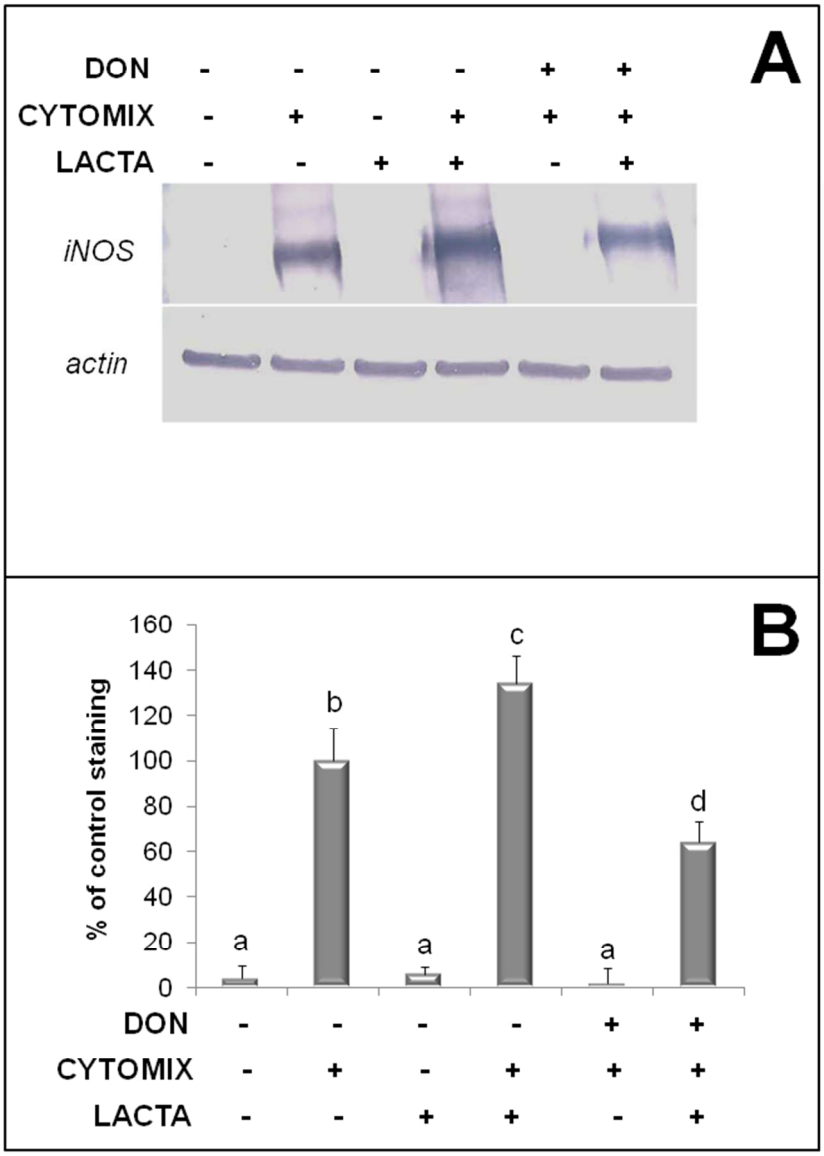

190x254mm (96 x 96 DPI)

Figure 9

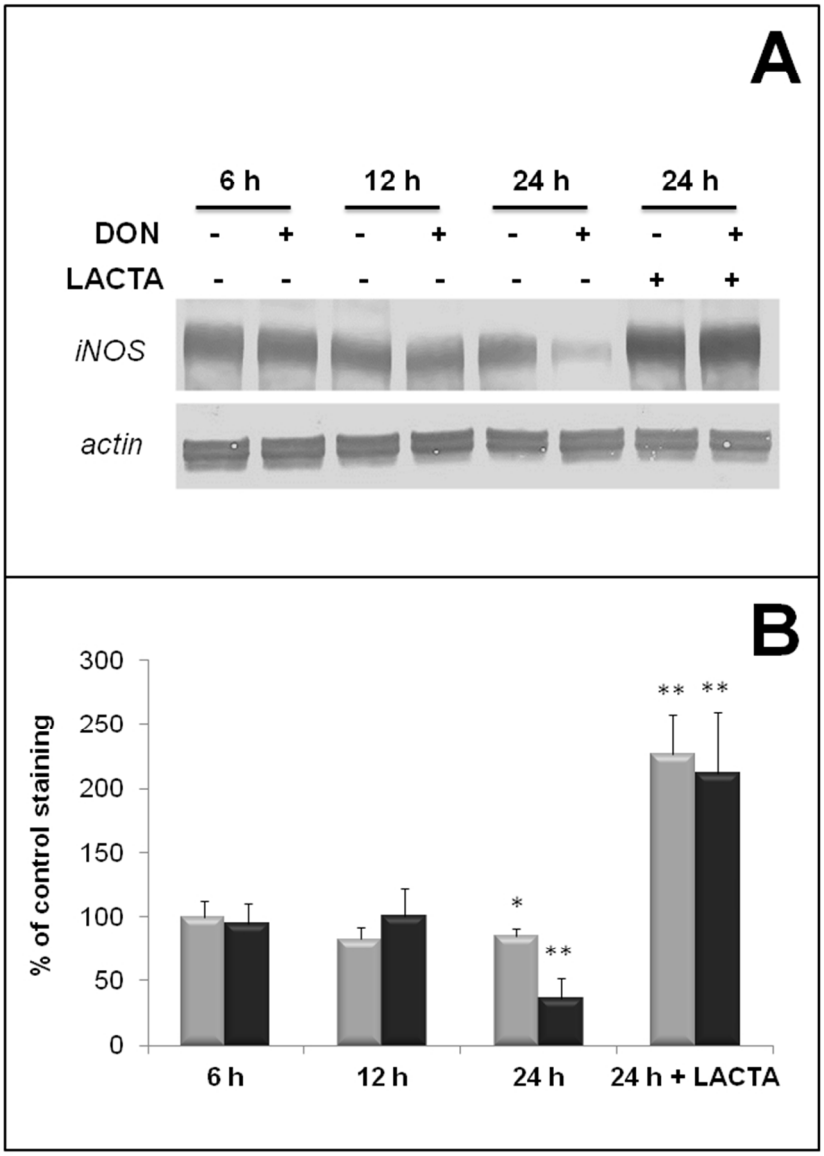

190x254mm (96 x 96 DPI)

Fig 10

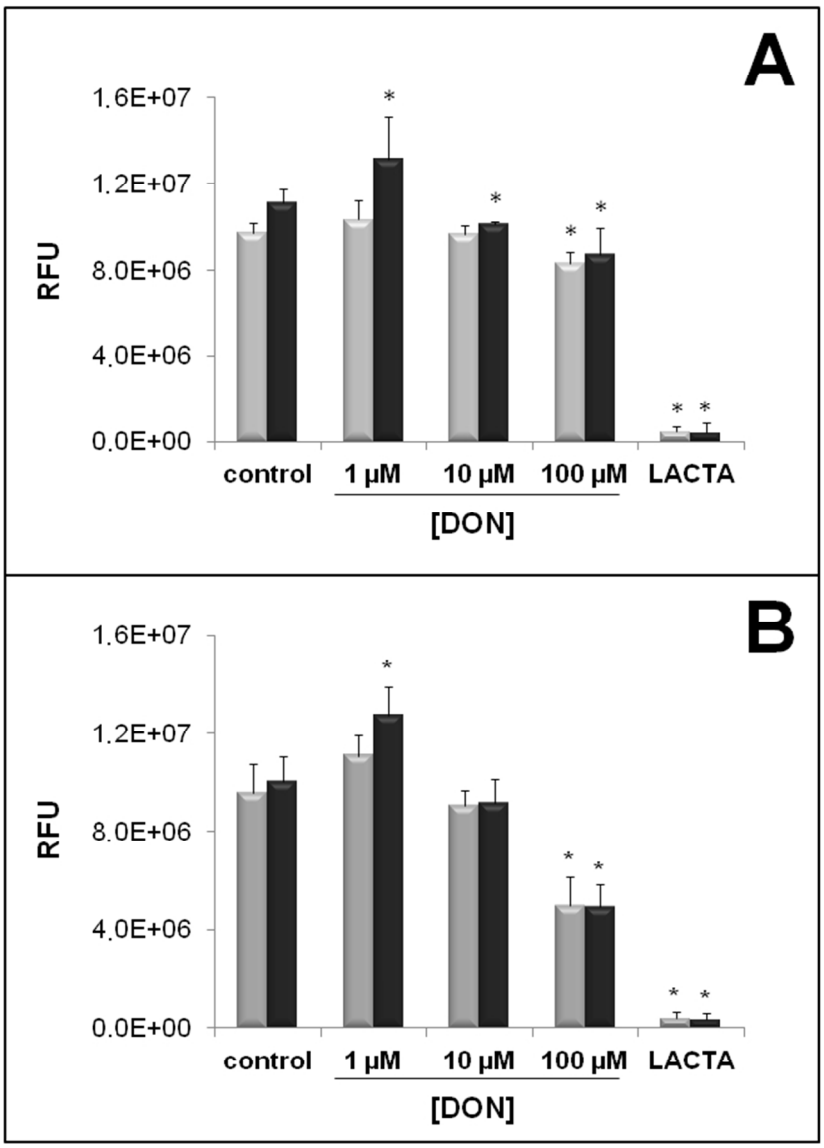

190x254mm (96 x 96 DPI)

Figure 11

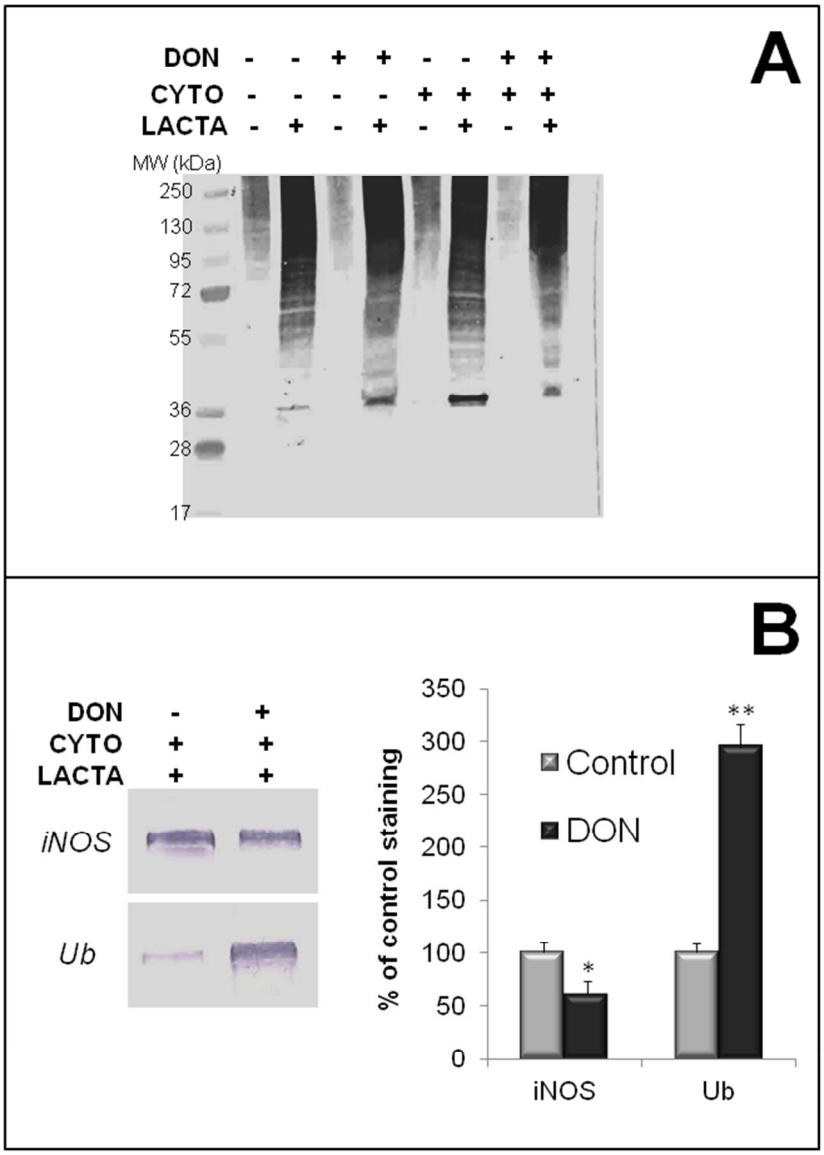

190x254mm (96 x 96 DPI)

Fig 12

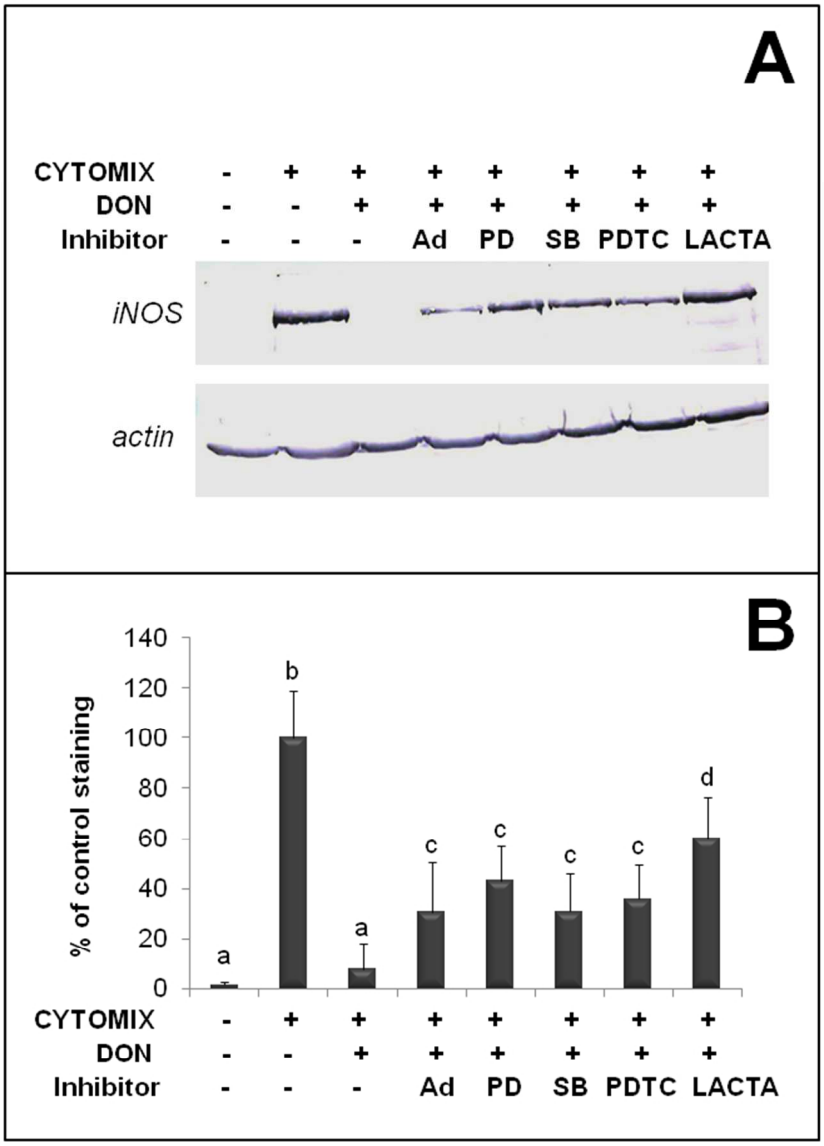

190x254mm (96 x 96 DPI)

Fig 13

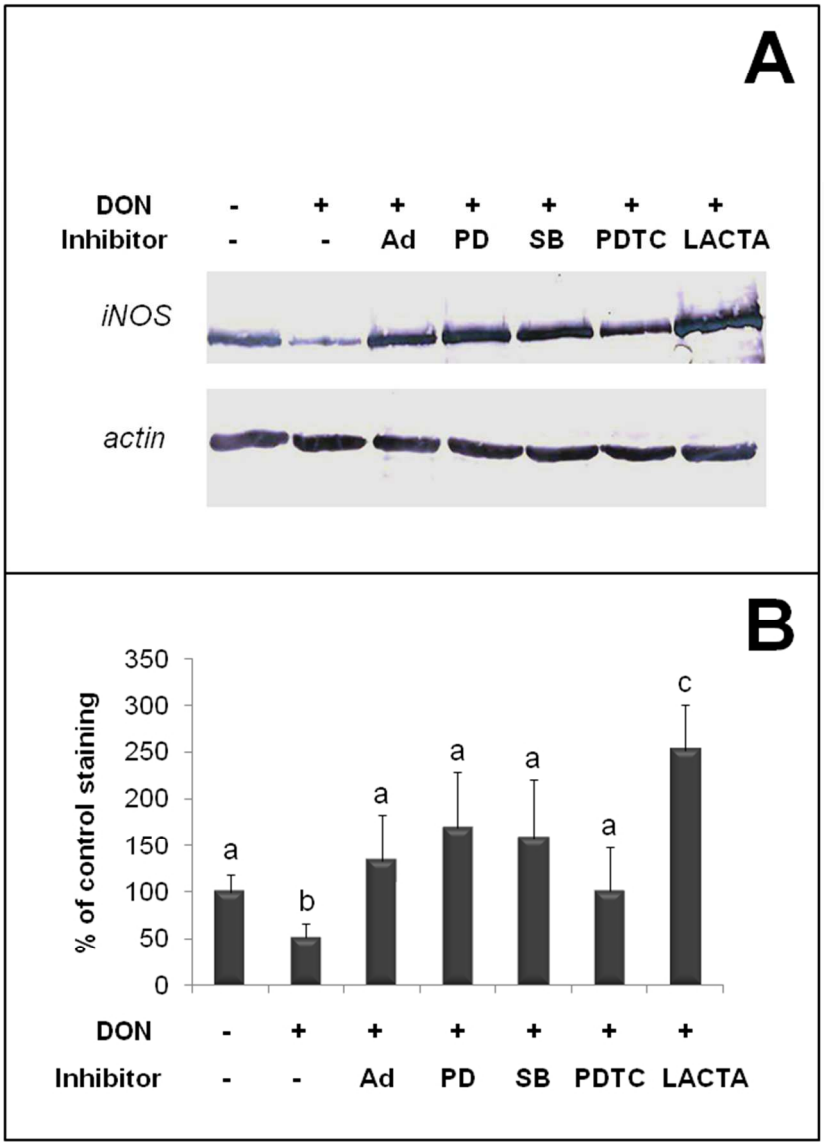

190x254mm (96 x 96 DPI)